Numerical Analysis of ICRF Minority Heating in Helitoron J*)

Hiroyuki OKADA, Kota NOMURA[1)], Hiroto WATADA[1)], Shinji KOBAYASHI, Hyunyong LEE[1)], Tohru MIZUUCHI, Kazunobu NAGASAKI, Takashi MINAMI, Satoshi YAMAMOTO, Shinsuke OHSHIMA[2)], Masaki TAKEUCHI, Shigeru KONOSHIMA, Takashi MUTOH[3)], Kiyofumi MUKAI[1)], Kento YAMAMOTO[1)], Masashige SUWA[1)], Hiroaki YASHIRO[1)], Hayao YOSHINO[1)], Yuji NAKAMURA[1)], Kiyoshi HANATANI and Fumimichi SANO

Institute of Advanced Energy, Kyoto University, Gokasho, Uji 611-0011, Japan
[1)] *Graduate School of Energy Science, Kyoto University, Gokasho, Uji 611-0011, Japan*
[2)] *Kyoto University Pioneering Research Unit for Next Generation, Gokasho, Uji 611-0011, Japan*
[3)] *National Institute for Fusion Science,322-6 Oroshi-cho, Toki 509-5292, Japan*

(Received 22 December 2010 / Accepted 21 April 2011)

The effect of the magnetic configuration on fast-ion confinement is one of the most important topics for helical devices. Fast-ion velocity distributions have been investigated using ion cyclotron range of frequencies (ICRF) minority heating in Heliotron J with special emphasis on the effect of the toroidal ripple (bumpiness) of the magnetic field strength. In measurements of the fast-ion tail generated by ICRF minority heating, a high bumpiness configuration is found to be preferable for tail formation. However, the measurement area based on the line of sight of the fast-ion detector was restricted in this experiment. Due to the complexity of the magnetic field in Heliotron J, three-dimensional analysis is required to interpret the experimental results. Monte-Carlo simulations were performed. The calculation results agree well with the experimental results for high-energy tail formation. The effective temperature of minority protons was estimated.

Keywords: fast ion confinement, magnetic configuration, ICRF, minority heating, Monte-Carlo simulation

DOI: 10.1585/pfr.6.2402063

1. Introduction

Fast-ion confinement is one of most important topics for helical devices since the alpha particle heating efficiency in a fusion reactor depends on the loss cone structure for fast ions in velocity space. In a non-axisymmetric confinement device such as Heliotron J [1–3] (see Fig. 1; $R_0 = 1.2$ m, $a = 0.1$-0.2 m, $B_0 \leq 1.5$ T), the orbits of trapped particles are very complex due to the three-dimensional magnetic field. The toroidal ripple (bumpiness) of the magnetic field strength is one of key parameters for enhancing confinement in the Heliotron J configuration [3]. The fast-ion velocity distribution has previously been investigated using fast protons generated by ion cyclotron range of frequencies (ICRF) proton-minority heating in Heliotron J with special emphasis on the effect of the bumpiness and the heating position [4–7]. In the present study, the role of the bumpiness is investigated by measuring fast ions generated by ICRF heating and by performing Monte-Carlo simulations. Initial results for Monte-Carlo simulations of fast ions have been obtained and the effects of the configuration have been discussed [6]. This paper presents energy spectra and compares the effective temperatures of minority ions.

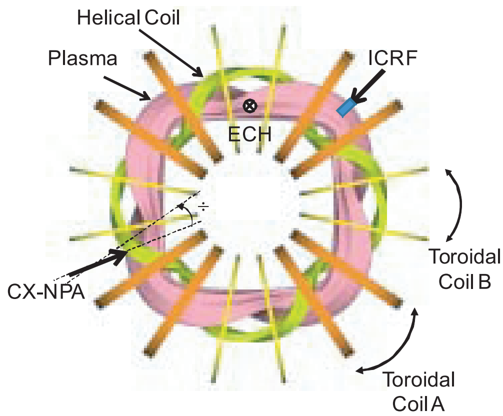

Fig. 1 Schematic top view of a plasma, a helical coil and two types of toroidal coils in Heliotron J. The major radius of the torus is 1.2 m. ICRF antennas are installed in the corner section. The toroidal position of the CX-NPA is almost opposite the ICRF antennas. The definition of the toroidal angle of line of sight for the CX-NPA is also illustrated.

The bumpiness can be varied by altering the ratio of the coil current of toroidal coil A to that of toroidal coil B in Fig. 1. The fast ions are measured using a charge-exchange neutral particle energy analyzer (CX-NPA) installed toroidally opposite the ICRF antennas. From these

author's e-mail: okada@iae.kyoto-u.ac.jp
*) This article is based on the presentation at the 20th International Toki Conference (ITC20).

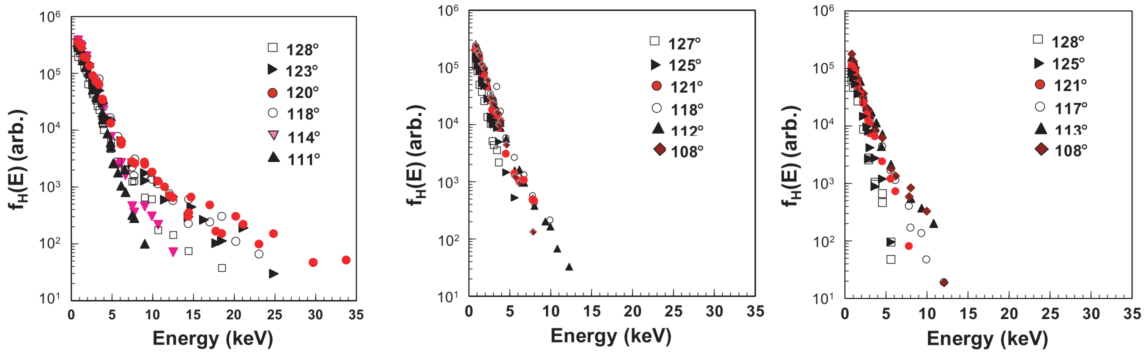

Fig. 2 Minority hydrogen spectra generated by ICRF heating at various pitch angles are measured by the CX-NPA for the (a) high, (b) medium, and (c) low bumpinesses. By varying the toroidal and poloidal angles of the CX-NPA, energy spectra were measured for the condition that the line of sight of the CX-NPA crosses the magnetic axis for all cases.

measurements, the dependence of the energy spectra on the pitch angle was obtained for bumpinesses (defined as B_{04}/B_{00}, where B_{04} is the bumpy component and B_{00} is the averaged magnetic field strength) of 0.01, 0.06 and 0.15 at $\rho = 0.67$.

An ICRF wave with a frequency of approximately 20 MHz was injected into electron cyclotron heated (ECH) plasmas in the central heating condition so that the minority cyclotron resonance layer is vertical in the poloidal cross section and intersects the plasma axis (see Fig. 3 of Ref. [6]). The magnetic field and the ICRF frequency are selected such that the ECH resonance is located on the plasma axis. The magnetic field is 1.25 T on the plasma axis in the ECH injection section, whereas the ICRF frequency is adjusted so as to satisfy the central heating condition for each bumpiness. The line-averaged electron density is $0.4 \times 10^{19}\,\mathrm{m}^{-3}$, the 70-GHz ECH injection power is 0.30-0.35 MW, and the ICRF injection power is 0.25-0.30 MW. The ion and electron temperatures at the center of the ECH plasma are about 0.2 and 0.8 keV, respectively. The majority and minority species of the plasma are deuterium and hydrogen, respectively. The minority ratio is about 10%. A CX-NPA is used to detect energetic ions. It can scan the line of sight in the toroidal direction from -10 to $+18°$ and in the poloidal direction from -3 to $10°$ to observe charge-exchange neutrals. Varying the toroidal angle will mainly alter the observed pitch angle. The distribution in the poloidal cross section can be measured by varying the poloidal angle. The CX-NPA has 10 channels for hydrogen and 10 channels for deuterium. An $E//B$ analyzer is used. The energy ranges are from 0.4 to 80 keV for hydrogen and from 0.2 to 40 keV for deuterium with a resolution of 4 to 10%.

2. Minority Energy Spectra in ICRF Heating Experiment

Good confinement of fast ions and high-efficiency of ICRF heating for a high bumpiness have been achieved [6, 7]. Figures 2 (a)-(c) show the pitch angle dependences

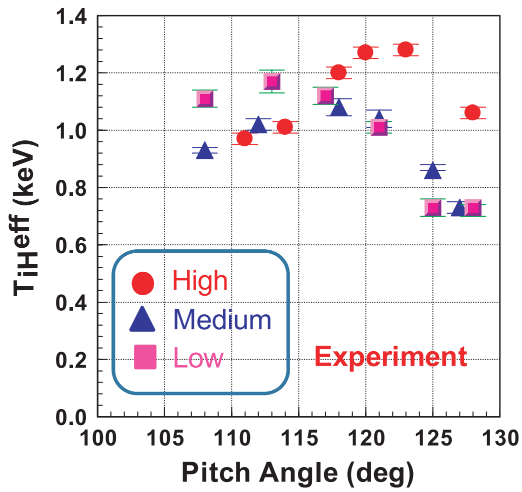

Fig. 3 Effective temperature of minority hydrogen estimated from the energy spectra for energy in the range from 1 to 7 keV for the three bumpinesses in Fig. 2.

of the energy spectrum for three different bumpinesses. Each figure shows results for energy spectra for six different pitch angles. The pitch angle dependence is obtained by varying mainly the toroidal angle such that the line of sight intersects the magnetic axis. The observed pitch angles lie within ± 5° of each chord. For the high bumpiness (Fig. 2 (a)), an ion flux is observed up to an energy of 34 keV at a pitch angle of 120°. Such high-energy particles were not observed at the medium and low bumpinesses. The highest tail was observed at an angle of about 30° relative to the perpendicular to the magnetic field. The tail component decreases as the angle decreases toward 90° (see Fig. 2 (a)). The tail also decreases as the pitch angle increases above an angle of 120° since there is no acceleration mechanism parallel to the magnetic field. For the medium and low bumpinesses, no fast ions are observed above 15 keV (see Figs. 2 (b) and (c)) and the dependence of the energy spectrum on the pitch angle also differs from that for the high bumpiness.

For quantitative comparison, the effective temperature

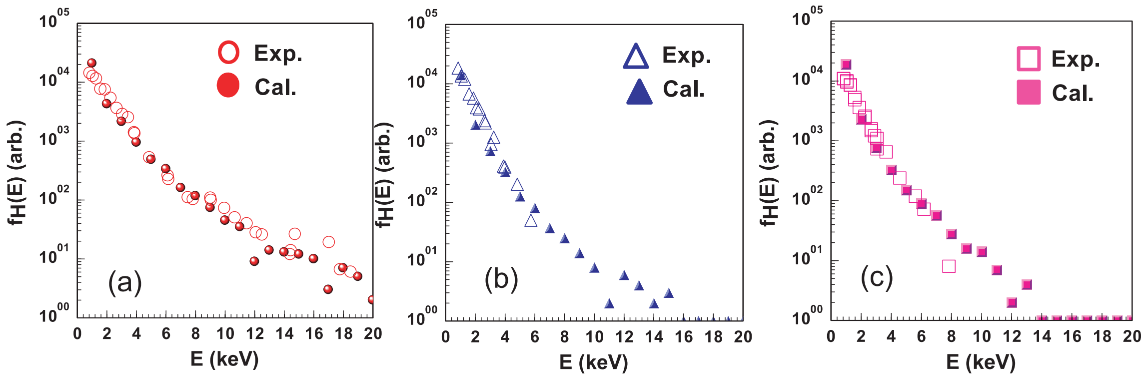

Fig. 4 The energy spectra calculated by Monte-Carlo method for three bumpiness cases are illustrated by solid symbols. The pitch angle range is 120 ± 5°. The experimental energy spectra obtained by CX-NPA measurements at 120° are indicated by open symbols. Results are shown for the (a) high, (b) medium, and (c) low bumpinesses.

of the minority high-energy tail is estimated from fast ions with energies in the range from 1 to 7 keV. The effective temperature clearly represents the changes in velocity space for the three bumpinesses (see Fig. 3). The maximum effective temperature is observed at a pitch angle of 120° for the high bumpiness (see Fig. 2 (a)). For each bumpiness, the effective temperature gradually decreases as the pitch angle decreases to its lowest value. There is known to be a relatively large loss region at a pitch angle of about 90° outside the torus in the corner section where ICRF antennas are installed. This loss region is thought to affect the fast-ion distribution in velocity space. The loss region is the smallest for the high bumpiness in this cross section. The confinement of trapped ions is improved due to the enhanced toroidal mirror component. However, it is difficult to estimate the overall effect of the loss region structure on fast-ion confinement because the structure varies with the position in a plasma column. In addition, the CX-NPA has a limited observation area. Numerical analysis using Monte-Carlo simulation is useful for establishing a physical model for the energy spectra in the three-dimensional magnetic field of Heliotron J.

3. Monte-Carlo Simulation Results

To interpret the experimental results and to determine the fast-ion distribution in a plasma volume, Monte-Carlo simulations were performed. The numerical model includes orbit tracing, Coulomb collisions [8], and acceleration [9] by ICRF heating. Minority protons are used as test particles and heating is simulated by the velocity kick in the perpendicular direction in velocity space when ions cross the cyclotron layer. In this calculation, the acceleration term for ICRF heating is proportional to the ICRF electric field amplitude, which is an input parameter. The electric field amplitude is determined from the input power for ICRF heating. Although it is possible to determine the heating profile as a function of the magnetic field, plasma parameters, and wave frequency, it is not simple to calculate the rf electric-field structure and the absorption profile for the magnetic configuration of Heliotron J. Here, the rf electric-field profile was assumed to be parabolic, as in previous calculations for Heliotron E plasmas [9]. The initial test ion distribution is uniform in the toroidal and poloidal directions and parabolic in the radial direction. The initial ion energy is randomly selected from the Maxwell distribution characterized by the bulk ion temperature.

Using 500,000 particles, the velocity distributions of the minority protons were calculated for the three bumpinesses. The plasma parameters are $T_e(0) = 0.7$ keV, $T_i(0) = 0.3$ keV, $n_e(0) = 0.5 \times 10^{19}$ m^{-3}, and $Z_{eff} = 3.0$. The input rf field is adjusted so that the input power is about 100 kW in each case. Orbit tracing with acceleration and collisions is performed for 2 ms. Under these conditions, the velocity distribution reaches steady state within 1 ms. All figures in the present study show the distribution at 1 ms since the particle number subsequently decreased gradually due to loss. The calculated particles are summed within some bounded region in velocity space. This bounded region is specified in term of the particle energy and the pitch angle in this calculation. Figures 4 (a)-(c) show typical calculated energy spectra at a pitch angle of 120° for the three bumpinesses. In these figures, the vertical axes show the logarithm of the ion counts in the bounded region. This pitch angle (120°) gives the largest energy tail observed in the CX-NPA measurements. The calculated and experimental values are indicated by solid and open symbols, respectively. The calculation reproduces the high-energy tail up to 20 keV, which was measured only in the high bumpiness case (see Fig. 4 (a)). No detectable data was obtained in the CX-NPA measurements for energies above 6 and 8 keV for the medium and low bumpinesses, respectively. The measured and calculated energy spectra are identical at energies below 10 keV for the medium and low bumpinesses. Thus, the experimental and calculation data agree in this experimental condition.

The upper row of Fig. 5 shows the energy spectra at various pitch angles for the three bumpinesses and the lower row shows the effective temperatures estimated from

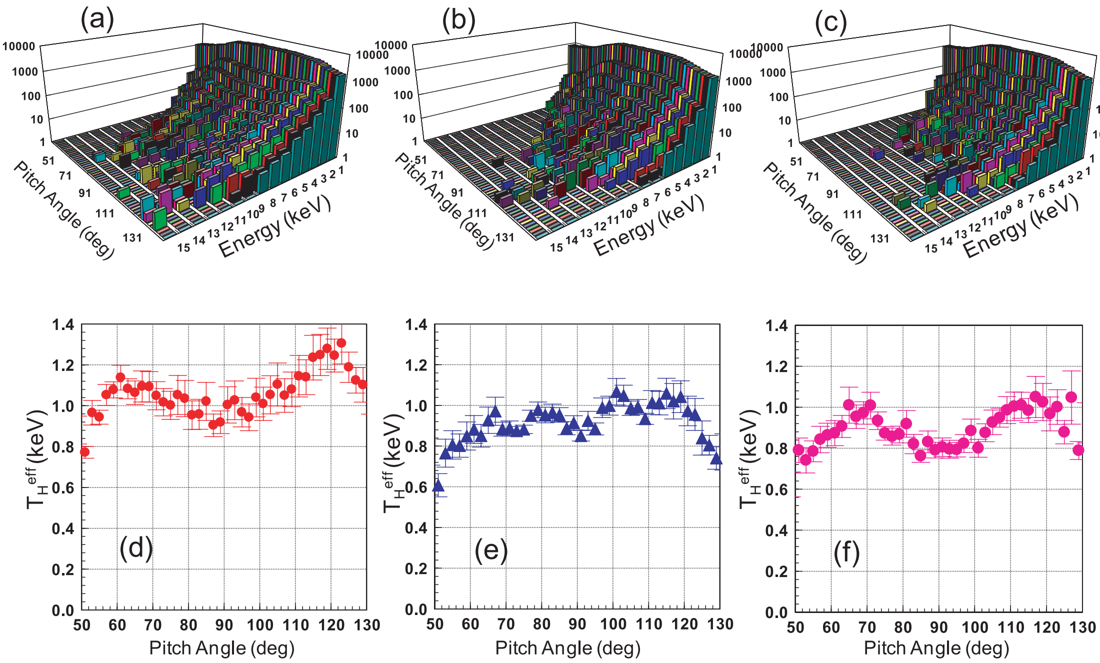

Fig. 5 Calculated pitch angle dependence of energy spectra for the (a) high (b) medium, and (c) low bumpinesses. 500,000 particles are used for each calculation. Spectra are calculated at pitch angle intervals of 2°. Effective temperature estimated from calculated energy spectrum in the energy range from 1 to 7 keV is illustrated for the (d) high, (e) medium, and (f) low bumpinesses.

the calculated energy spectra. Figure 5 (a) shows the relation between the calculated energy spectra and the pitch angle for the high bumpiness. The high bumpiness gives the largest energy-tail. The energy spectrum is calculated at pitch angle intervals of 2°. High-energy ions are observed at 90°, but there are not very many. High-energy ions are observed at pitch angles of 60 and 120°. The results are asymmetric about a pitch angle of 90°. The tail near 120° is larger than that near 60°. In the experiment, a high-energy tail is observed for the high bumpiness and it has a peak near 120° (see Fig. 2).

The medium bumpiness has a small tail (see Fig. 5 (b)). The fast-ion distribution below 10 keV is almost constant between 70 and 120°. The energy spectra vary little in this pitch angle range (see Fig. 2). The low bumpiness gives the smallest tail component (see Fig. 5 (c)). However, the results are asymmetric about a pitch angle of 90°. The high-energy component decreases as the pitch angle increases from 70 or 110° toward the perpendicular direction. It also decreases rapidly in the parallel and antiparallel directions. In the experiment results shown in Fig. 2, the number of fast ions increases toward 90°, whereas it is almost constant in the range from 108 to 117°.

The lower row of Fig. 5 shows the effective temperatures estimated from the calculated energy spectra. The effective temperature for the high bumpiness (see Fig. 5 (d)) has two peaks at 60 and 120° and it is the highest for the three bumpinesses at almost all pitch angles. For the medium bumpiness (see Fig. 5 (e)), the effective temperature has small peaks at 67, 80, 100 and 115°. In the experimental data shown in Fig. 3, s peak is observed at 118° and it gradually decreases toward 108°. The effective temperature for the low bumpiness (see Fig. 5(f)) is the lowest for the three bumpinesses. It has peaks at 70 and 110° and decreases near 90°, just as for the high bumpiness. Figure 6 shows the pitch angle dependence of the effective temperature of the minority fast ions obtained by the Monte-Carlo simulation for comparison with the experimental data in Fig. 3. The two results are consistent except for the low bumpiness for pitch angles in the range from 108 to 117°. In this region, the absolute value differs, although the pitch

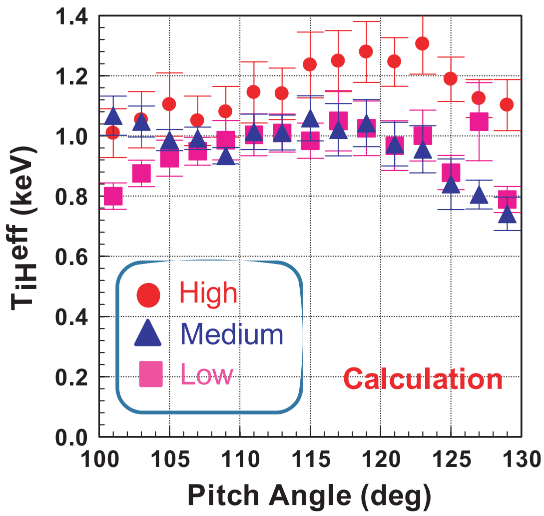

Fig. 6 Calculated effective temperature estimated in the energy range from 1 to 7 keV for the three bumpinesses is shown for comparison with Fig. 3.

angle dependences are almost identical.

4. Summary

The effect of the bumpy component of the magnetic field in Heliotron J has been investigated using ICRF minority heating. Measurements of the fast minority particle flux using a CX-NPA reveal that fast ion generation and confinement are most effective at a high bumpiness. The energy spectrum and the resultant effective temperature depend on the pitch angle. The largest high-energy tail is observed at an angle of about 30° relative to the normal. A Monte-Carlo code that includes an ICRF heating term has been developed to interpret experimental results and to develop a model for optimizing fast-ion confinement in a three-dimensional magnetic field. The calculation results are consistent with the experimental results for tail formation and the pitch angle dependence. The model used in the Monte-Carlo code is considered to be useful for analyzing fast ions in Helitoron J plasmas.

Acknowledgments

This work is performed with the support and under the auspices of the Collaboration Program of the Laboratory for Complex Energy Processes, Institute of Advanced Energy, Kyoto University, the National Institute for Fusion Science (NIFS) Collaborative Research Program (NIFS04KUHL002 and NIFS04KUHL030), and JSPS KAKENHI 22560819.

[1] F. Sano *et al*., J. Plasma Fusion Res. SERIES **3**, 26 (2000).
[2] T. Obiki *et al.*, Nucl. Fusion **41**, 833 (2001).
[3] M. Wakatani *et al.*, Nucl. Fusion **40**, 569 (2000).
[4] S. Kobayashi *et al.*, IAEA-CN-116/EX/P4-41 (2004).
[5] H. Okada *et al.*, Fusion Sci. Technol. **50**, 287 (2006).
[6] H. Okada *et al.*, Nucl. Fusion **47**, 1346 (2007).
[7] H. Okada *et al.*, Proc. 22nd IAEA Fusion Energy Conference, EX/P6-28 (2008).
[8] A.H. Boozer and G. Kuo-Petravic, Phys. Fluids **24**, 851 (1981).
[9] H. Okada *et al.*, Nucl. Fusion **36**, 465 (1996).